Available online at www.sciencedirect.com
SCIENCE DIRECT®
Applied Acoustics 67 (2006) 487–510
applied acoustics
www.elsevier.com/locate/apacoust

# Parameter study of sound propagation between city canyons with a coupled FDTD-PE model

T. Van Renterghem [a,*], E. Salomons [b], D. Botteldooren [a]

[a] Ghent University, Department of Information Technology, Sint-Pietersnieuwstraat 41, B-9000 Gent, Belgium
[b] TNO Science and Industry, P.O. Box 155, 2600 AD Delft, The Netherlands

Received 28 July 2005; received in revised form 26 September 2005; accepted 28 September 2005
Available online 10 November 2005

**Abstract**

A parameter study is performed for the case of two-dimensional sound propagation from a (source) city canyon to a nearby, identical (receiver) city canyon. Focus was on sound pressure levels, relative to the free field, in the shielded canyon. An accurate and efficient coupled FDTD-PE model was applied, exploiting symmetry of the source and receiver canyon. With the proposed calculation method, simulations were necessary in only half the sound propagation domain. The shielding in the receiver canyon in case of a coherent line source was compared to the shielding by an incoherent line source, by means of sound propagation calculations in a number of 2D cross-sections through source and receiver. It was found that the shielding is rather insensitive to the width-height ratio of the canyons. The presence of diffusely reflecting façades and balconies lead to an important increase in shielding compared to flat façades. Rigid façades yield significantly lower shielding compared to partly reflecting façades. Effects of a moving atmosphere were modeled in detail. Shielding decreases significantly in case of downwind sound propagation when comparing to sound propagation in a non-moving atmosphere. Refraction is the most important effect in the latter. In case of upwind sound propagation, turbulent scattering plays an important role and the shielding is similar to the one of a non-moving atmosphere for the parameters used in this paper. The combination of effects, as is shown by some examples, is in general not a simple addition of the separate effects.


*Keywords:* City canyons; Moving atmosphere; FDTD; PE

* Corresponding author.
*E-mail address:* Timothy.Van.Renterghem@intec.Ugent.be (T. Van Renterghem).

0003-682X/$ - see front matter © 2005 Elsevier Ltd. All rights reserved.
doi:10.1016/j.apacoust.2005.09.006

## 1. Introduction

Noise annoyance in urban areas is a major issue. In a city, there is a combination of a large number of sound sources and a large number of inhabitants. Traffic noise is generally accepted to be the major noise source. Commonly used noise reducing measures for the latter like noise barriers are often not applicable in city centers. Well informed city planning, with knowledge of the factors that influence sound propagation in urban environments, is therefore of major importance.

Sound propagation calculations in urban areas focus mainly on sound propagation along streets (and into side streets). Applications of ray-tracing techniques (and improved variants thereof) are numerous. Simulations for various street geometries were performed in [1], in order to produce look-up tables. In [2], interference effects are included in ray-tracing calculations. The understanding of the importance of diffuse reflection on building façades led to the development of models based on the principle of radiosity [3,4] and models based on the linear transport equation and diffusion equation [5,6].

Based on noise annoyance surveys, it was found that easy access to a quiet place in a noisy area reduces the percentage highly annoyed residents [7]. The preservation of silent places in a city (like backyards) can therefore help to reduce the city noise problem [8].

The centers of large urban areas consist of a number of confined spaces, enclosed by tall buildings. These are often called ''city canyons''. Accurate calculations of sound propagation from a source canyon (e.g. a street) towards a shielded, receiver canyon is of interest from the viewpoint of the quiet sides. Such calculations are rather difficult, and there is a trend to overestimate the shielding with present models [9]. Recently, the equivalent sources method (ESM) [10] was applied with success to model sound propagation between city canyons.

Formulations like the ESM (and the boundary element method), based essentially on the Green's function, fail however when the sound propagation medium is moving and/or inhomogeneous. The applicability of these methods is limited since the effects of refraction are often important. With the ESM method it is possible to model a turbulent atmosphere by accounting for the loss in coherence between the different sound paths to a single receiver, however in a non-refracting atmosphere [11].

At present, the finite-difference time-domain method (FDTD), solving the moving-medium sound propagation equations [12–14], can be considered as a complete model, taking into account the combined effect of multiple reflections, multiple diffractions, (inhomogeneous) absorbing and (partly) diffusely reflecting surfaces, in combination with a moving, non-homogeneous and turbulent atmosphere.

Scale modeling of sound propagation in a city street canyon in [15] revealed that the combination of various noise abatement approaches is complex and cannot be predicted by a simple addition of the individual effects. Numerical simulations with a model like FDTD are therefore useful.

The computational resources needed for FDTD simulations are however large. In this paper, this is (partly) overcome by using a coupled FDTD-PE (PE = parabolic equation) model [16], which has shown to drastically reduce computing times and memory use [16]. Simulations in 3D can only be performed for (very) low frequencies because of the lack of sufficient computational resources. It seemed therefore more interesting to use a 2D grid, while considering all relevant frequencies present in traffic noise. The source canyon and

receiver canyon are assumed to be geometrical identical in this paper. Calculations times are further reduced by exploiting this symmetry.

This paper is outlined as follows. In a first part, the computational methods are discussed briefly. It is indicated how the geometrical symmetry of the source and receiver canyons is exploited. In a second part, a parameter study is performed. A standard configuration is defined for comparison. The approach to reduce computing times and memory use in this paper is checked with FDTD calculations applied to the full computational domain. Focus is on sound pressure levels, relative to the free field (indicated by relative sound pressure levels), in the shielded canyon. The shielding of a coherent line source is compared to the shielding of an incoherent line source. The influence of the width–height ratio of the canyons and the degree of reflection near the walls is investigated. Calculations with completely flat façades are compared to calculations with partly diffusely reflecting façades. The influence of different forms of balconies, as well as the influence of a moving atmosphere, is studied both in downwind and upwind conditions. In a next section, the relative effect of some parameters in case of symmetric and asymmetric source–receiver locations is compared. In a last part, some simulations are performed with combinations of parameters.

## 2. Calculation method

### 2.1. General

For the parameter study, the two-dimensional idealized configuration as shown in Fig. 1 is used. The FDTD-PE model [16] is well suited for the calculations in the present configuration. In the complex source region (source canyon), FDTD is applied. PE is used to simulate sound propagation above the roofs, where the requirements for this model are fulfilled: we can assume one-way sound propagation, and the wind is directed mainly horizontally.

The approach that was followed for the calculations in this paper is illustrated in Fig. 1. When using a broadband source, only a single FDTD calculation is needed in the source canyon (grey area). At a short distance from the canyon edge, time signals are recorded on

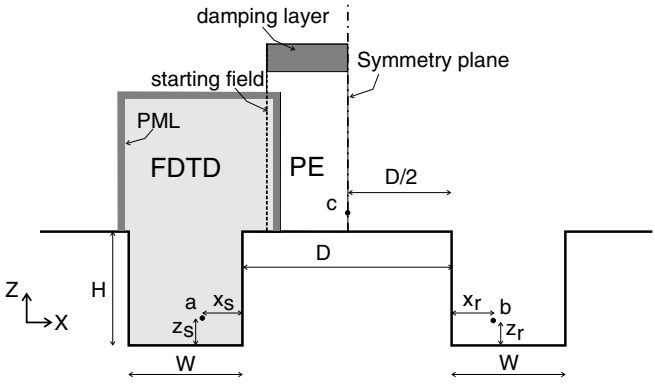


Fig. 1. Set-up of the coupled FDTD-PE model, exploiting symmetry. The FDTD and PE region are shown, with the starting field, close to the canyon edge. The canyon height is indicated with $H$, the canyon width with $W$ and the distance between the source and receiver canyon with $D$. The source is located at point $a$, the receiver at point $b$. Point $c$ is located at limited height on the symmetry plane.

a vertical array to generate starting functions for the PE method, using a transition from the time domain to the frequency domain by means of FFT. Finally, PE calculations are performed up to a receiver at the symmetry plane, for the frequencies of interest. Details of the FDTD-PE coupling can be found in [16].

The transfer function from location $a$ (source) to location $b$ (receiver) is approximately equal to the sum of the transfer function from $a$ to $c$ (intermediate receiver on the symmetry plane above the roofs) and the transfer function from $c$ to $b$. The argument for this approximate equality is simply that the transfer function from $a$ to $c$ involves one edge diffraction, while the transfer function from $a$ to $b$ involves two edge diffractions. Since the transfer functions between $a$ and $c$ and between $c$ and $b$ are equal (by the symmetry in Fig. 1 and by reciprocity), the transfer function from $a$ to $b$ is approximately equal to twice the transfer function from $a$ to $c$. An important condition is that $x_s$ must equal $x_r$ and $z_s$ must equal $z_r$.

This simple approach ignores, however, that the reflection on the roof is counted twice when doubling the transfer function from $a$ to $c$. This must be compensated for, as described in Section 3.3. This approach is similar to the one used in [17].

Full FDTD calculations (i.e., FDTD applied completely from source to receiver) are possible as well, but at a larger computational cost. When the conditions to exploit symmetry are not met, e.g., when investigating asymmetric source–receiver locations (see Section 3.5.7), full FDTD calculations will be performed.

### 2.2. FDTD and PE

The FDTD method (in 2D) is used to evaluate the moving-medium sound propagation equations in the source region. Perfectly matched layers are applied at the left and right boundaries (above the buildings), as well as at the upper boundary of the FDTD computational domain, to simulate an unbounded atmosphere [13].

In absence of flow, the efficient staggered spatial and staggered temporal grid is used [18]. In a moving medium, a stationary flow field is simulated with the CFD software Fluent [19]. Next, sound propagation calculations in a so-called background flow are performed. Staggered-in-space calculations are combined with the prediction-step staggered in time (PSIT) approach. The flow velocities used in this paper are sufficiently low to perform accurate calculations with the PSIT scheme. Details on this numerical scheme can be found in [20,21]. The impedance modeling approach proposed in [18] is used to simulate partly reflecting surfaces.

The Green's function PE model is applied (GF-PE) [22–24]. Two-dimensional calculations are performed.

## 3. Parameter study

### 3.1. Standard configuration

Sound propagation between two-dimensional city canyons is simulated. A two-dimensional simulation space implies an infinitely long source canyon and receiver canyon. An infinitely long, coherent line source is present in the source canyon.

The standard configuration is defined as follows. All buildings have a height ($H$) of 10 m. The canyon width ($W$) is 10 m. The distance between the canyons ($D$) is chosen to be 100 m.

All vertical planes (façades) are flat (specularly reflecting), and have a locally reacting normalized, real, frequency-independent surface impedance of 10. Horizontal planes like the street coverage and roofs are rigid. We are interested in traffic noise immission, after propagation towards a shielded canyon. Therefore, calculations up to the 1/3 octave band of 1250 Hz seemed sufficient. Due to these rather low frequencies and limited propagation distances, atmospheric attenuation is not accounted for, all the more since we are interested in sound pressure levels relative to the free field. The atmosphere is homogeneous and non-moving in the standard configuration. The source and receiver are somewhat displaced from the center of the canyons. The distances $x_s$ and $x_r$, as defined in Fig. 1, equal 4 m, while the heights above the ground $z_s$ and $z_r$ are chosen to be 1 m. Only the parameters that are different from the standard configuration are mentioned in the remainder of this paper.

Sound waves that travel back from the receiver canyon to the source canyon and then propagate again from the source canyon to the receiver canyon can be neglected for the chosen set of parameters. The geometric attenuation caused by the large distance between the canyons ($D$) would result in very small contributions relative to the first propagation from the source canyon to the receiver canyon.

### 3.2. Computational parameters

The origin of the $xz$ coordinate system is placed in the center of the source canyon, at street level. The FDTD computational domain extended from $-7\text{ m} < x < 11\text{ m}$ in horizontal direction, and from $0\text{ m} < z < 51\text{ m}$ in vertical direction. The lowest frequency of interest is the lower boundary of the 50 Hz 1/3 octave band namely 44 Hz. The highest frequency of interest is the upper boundary of the 1250 Hz 1/3 octave band namely 1405 Hz. A spatial discretization step of 0.025 m resulted in about 10 computational cells per wavelength for the latter. The temporal discretization step was 5.19 μs. This results in a 2D-CFL number (for square cells) near 1, which is most efficient for numerical accuracy and computing time [18]. The perfectly matched layers at the boundaries of the domain consisted of 40 computational cells, and absorption parameters were optimized such that a sound wave is reduced by 120 dB upon reflection at normal incidence. A broadband asymmetric Gaussian pulse is emitted at the source position. The center frequency was 730 Hz, the 3 dB-bandwidth equaled 500 Hz. The simulation times were chosen long enough to capture all significant reflections in the source canyon. After 15,000 time steps, sound pressure levels did not change anymore in the standard configuration as described in Section 3.1.

The starting function for PE is located at 4 m from the edge of the middle building ($x = 9$ m in the standard configuration).

20 frequencies per 1/3 octave band were calculated with PE. The vertical grid spacing was one tenth of the wavelength. For the horizontal grid spacing we used 5 times the wavelength. For all frequencies, the height of the PE grid was 4096 grid spacings, including an absorbing top layer of 1500 grid spacings.

### 3.3. Accuracy

In this section, we show that the approach followed in this paper is accurate. FDTD calculations from the source to the receiver canyon (=reference calculations) were compared to calculations following the approach described in Section 2.1.

At sufficient distance from the source, sound pressure levels were quite independent of height above the roof top (at limited heights). The intermediate receiver is taken at a height of 2 m above the roof.

Very good agreement between the reference calculation and the solution obtained by doubling coupled FDTD-PE calculations at the symmetry plane is found. A correction needs to be applied since reflection on the roof is counted twice in our approach [25]. When propagating directly from the source to the receiver, the diffracted wave will only reflect once on the roof. Since we are simulating a rigid roof, 6 dB needs to be subtracted from the doubled relative sound pressure levels at the symmetry plane. This correction is independent of frequency and of the geometry of the source/receiver canyon.

In Fig. 2, the full spectrum of sound pressure levels, relative to free field calculations, is shown. PE calculations are performed with a resolution on the frequency axis of 1 Hz. The standard configuration as described in Section 3.1 is used. The very resonant behavior of the configuration under study becomes clear. Deviations between full-FDTD calculations and the proposed, simplified approach can only be observed near the deep, destructive inferences. In Fig. 3, the same comparison is presented in 1/3 octave bands.

### 3.4. Incoherent line source

Noise from a traffic stream is commonly modeled as an incoherent line source. A point source in a 2D simulation space however is equivalent to a coherent line source in 3D. The difference between a coherent and incoherent line source in the standard configuration is therefore examined. By expressing results in 1/3 octave bands, interference effects from a coherent line source will already be partly averaged out.

To examine the influence of source coherence, the following pseudo-3D approach is used. The incoherent line source in the street canyon is discretized in a number of point

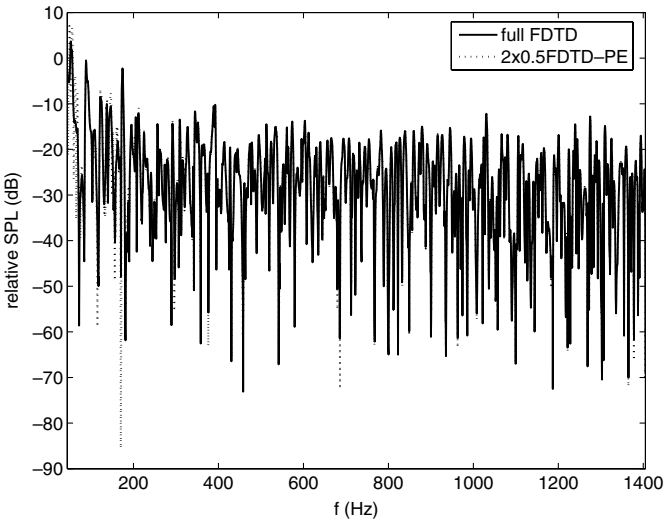


Fig. 2. Relative sound pressure levels in the receiver canyon, calculated with FDTD completely from source to receiver, and with the FDTD-PE approach exploiting symmetry.

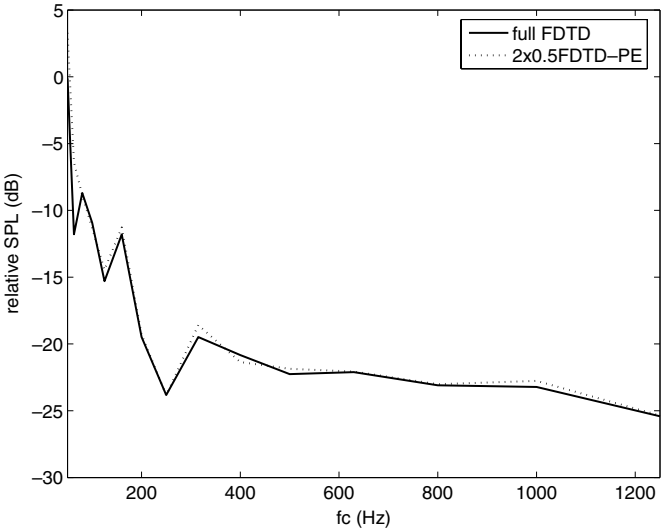


Fig. 3. Relative sound pressure levels in the receiver canyon, expressed in 1/3 octave bands (indicated by their center frequency $f_c$), calculated with FDTD completely from source to receiver, and with the FDTD-PE approach exploiting symmetry.

sources (see Fig. 4). For each point source, a calculation is performed in a vertical plane through the source and receiver. This approach uses the excess attenuation equivalence between a coherent line source (point source in 2D) and a point source in 3D, as shown in [16]. In the next step, the relative sound pressure levels from the different sources are averaged out energetically. This means that a 3D incoherent line source is modeled by performing a number of 2D simulations, with different canyon widths.

In this approach, it is implicitly assumed that all buildings façades are oriented orthogonal to the different cross-sections where a calculation is done. The ''turning'' of the façades is an approximation.

Relative sound pressure levels in case of a coherent and an incoherent line source are compared in Fig. 5. The standard configuration as described in Section 3.1 is used. The line source is represented by 11 equidistant point sources. Due to symmetry, sound propagation calculations for only 6 different canyon widths were necessary. The angle $\phi$ (see Fig. 4) ranged from 0° to 70°, corresponding to canyon widths ranging from 10 to 30 m, respectively.

Sound propagation in case of different canyon widths results in a shift of the frequencies where interference is observed. The interference minima will therefore be less pronounced when averaging the different contributions to the receiver. As a result, the shielding will be smaller compared to a coherent line source. This effect is clearly seen in Fig. 5, for the 1/3 octave band values.

### 3.5. Results

Results of sound propagation from the source canyon towards the receiver canyon in the standard configuration were shown in Fig. 3. At very low frequencies, sound pressure

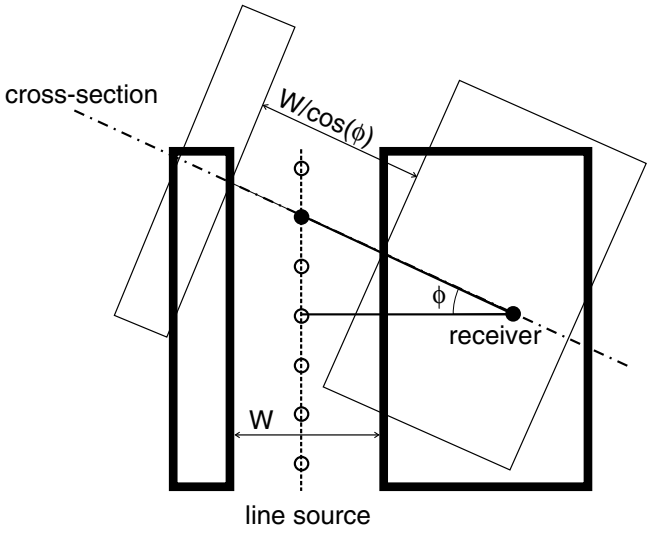


Fig. 4. Top view of the canyon configuration, indicating how an incoherent line source is modeled in a 2D approach.

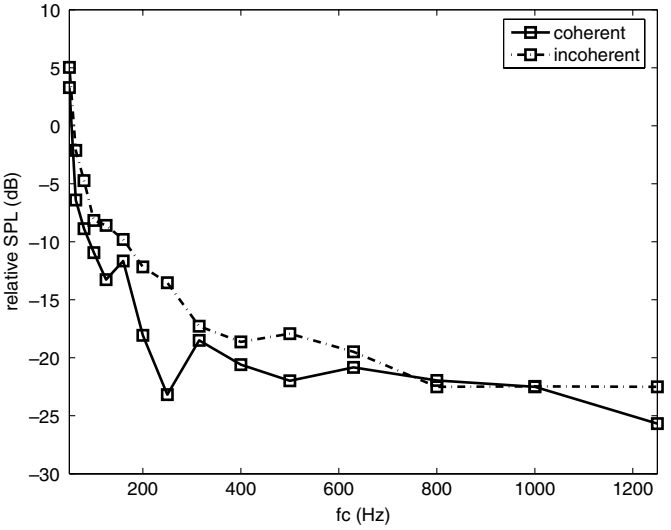


Fig. 5. Relative sound pressure levels in the receiver canyon, in case of a coherent and an incoherent line source.

levels relative to free field calculations are close to zero. There are multiple reflections on the façades and street ground, and consequently multiple diffraction paths to the receiver. Since low frequencies are diffracted to an important degree, almost no shielding is observed relative to free field calculations. With increasing frequency, sound is diffracted to a lesser degree and shielding increases.

In this section, some important parameters are investigated.

*3.5.1. Canyon width–height ratio*

Width–height ratios ($W/H$) of 0.5, 1, 1.5 and 2 are simulated. The canyon height is in each case 10 m. Results are shown in Fig. 6. The source and receiver are located in horizontal direction at 1 m from the canyon center, towards the middle building. The source height and receiver height are in each case 1 m. The distance between the canyons $D$ is fixed.

The shielding of the narrow canyon ($W/H = 0.5$) is large. With increasing $W/H$ ratio the relative sound pressure levels in the receiver canyon increase. When the width of the canyon exceeds its height, the sound pressure levels become more or less constant.

The angles of the first diffractions (those that did not interact with the façades) on the edge of the middle building are larger for narrow canyons than in case of a wider canyon, which is beneficial as regards shielding. On the other hand, there is less geometrical spreading in between multiple reflections between the façades in a narrow canyon. So reflected waves that arrive later on have larger amplitudes when reaching the building edge. The first mechanism dominates in the narrow canyon. For wider canyons, both effects seem to cancel out.

Linear scaling can be applied to the configuration under study. When considering other canyon heights, but the same W/H ratios, the same relative sound pressure levels are obtained at scaled frequencies. Note that the source position and the distance between the canyons must be scaled as well.

*3.5.2. Façade reflection*

The effect of façade reflection is investigated. As an idealization of common building materials, locally reacting materials described by a real, frequency-independent surface

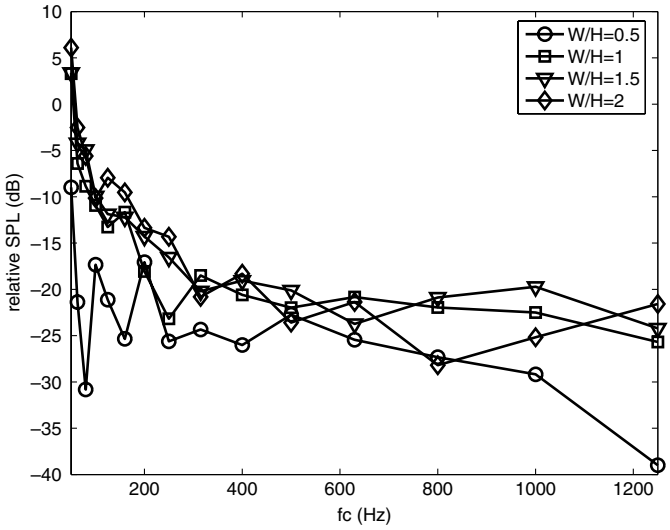


Fig. 6. Relative sound pressure levels in the receiver canyon, for different width/height ratios of the canyons.

impedance are modeled in this section. Frequency-dependent impedances, with non-zero imaginary parts, can be simulated in FDTD as shown in [18,26].

Normalized impedances of 5 and 10 are simulated, as well as a perfectly reflecting façade. The corresponding reflection coefficients at normal incidence are 0.67, 0.82 and 1. These values are applied to the complete façade height. Results are shown in Fig. 7. The shielding towards the receiver canyon in case of perfectly reflecting façades is very poor. The effect of decreasing the degree of reflection (to $Z = 10$, which is typical for bricks) is very large, because of the large number of interactions between the façades. A difference of 20 dB is observed. Sound pressure levels in the receiver canyon decrease further when making the walls less reflecting. The presence of large areas of glass, which is typical of modern buildings, is therefore not beneficial in the view of quiet sides.

### 3.5.3. Diffuse reflection

Façades of real buildings are not flat, and consist of smooth planes broken up by protrusions and recesses due to features such as windows, doors and architectural details [27]. Diffuse reflection in urban situations is important because of the large number of reflections between façades in a street canyon. A commonly used method to account for diffuse reflection is assuming that a certain amount of energy is transferred from the specular (coherent) field to the diffuse field with each reflection. The scattering coefficient quantifies this transfer. The values commonly used in such models are small, and are in the range 0.1–0.3 [1,27].

It was shown by theoretical considerations that the diffuse mechanisms will tend to dominate for all but the lowest orders of reflection [27]. The use of a scattering coefficient assumes that façades scatter randomly from every point. In reality however, diffusers are well-localized.

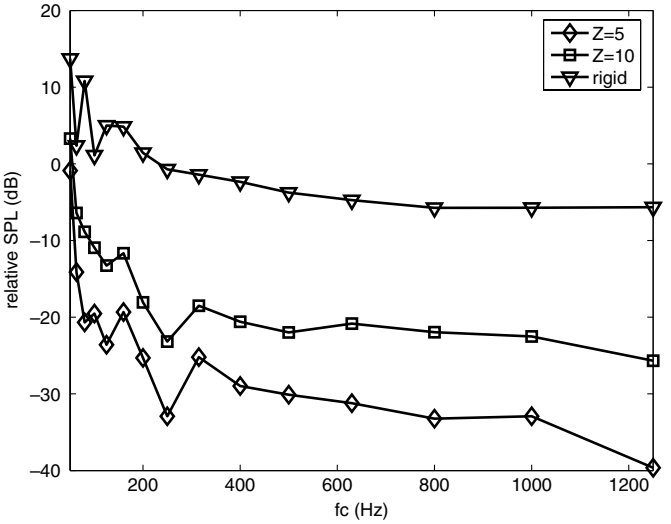


Fig. 7. Relative sound pressure levels in the receiver canyon, for flat façades with a (uniform) normalized impedance of 5 and 10, as well as for a completely rigid façade.

Modeling localized diffusers is rather easy in FDTD. Diffuse reflection is explicitly modeled by making surfaces irregular. This approach does not induce any difficulties in the FDTD method that was used, and does not result in a need for extra computational resources. In a structured, Cartesian grid, the finest roughness element near the façade is as small as the spatial discretization step. Recesses and protrusions due to windows and window sills are modeled near a façade, as well as a rough wall. This profile is shown in detail in Fig. 8. The windows itself and the window sills are rigid, while the rest of the façade has a normalized, real impedance of 10.

In Figs. 10 and 11, a number of snapshots of the sound pressure field (in dB) are shown, in case of flat façades and in case of the profiled façade shown in Fig. 8. A broadband pulse was excited at the source location. The progression from a coherent sound field to a complete diffuse field is clearly visible in case a diffusely reflecting façade is present.

The effect of introducing diffuse reflection on sound pressure levels in the receiver canyon is presented in Fig. 12. For comparison, calculation results for a fully flat façade are shown for $Z = 10$, for a rigid surface and also for a combination of these impedances (as shown in Fig. 9).

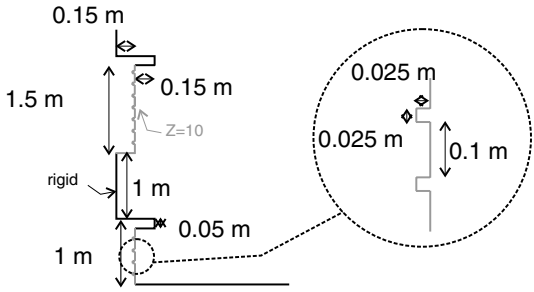


Fig. 8. The profiled façade that is used for the simulations. Recesses by windows (rigid) and protrusions by window sills (rigid) are shown, together with a detail of the rough wall. The non-rigid parts of the façade have a normalized, real impedance of 10.

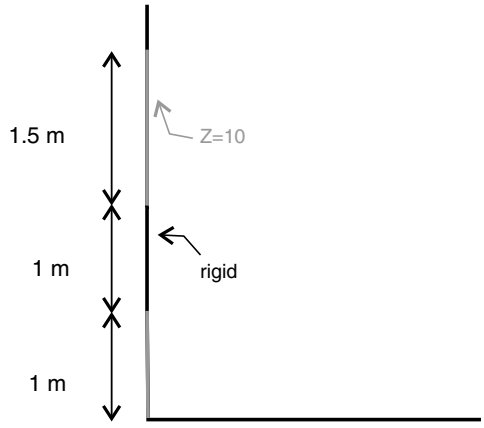


Fig. 9. The equivalent flat façade of Fig. 8 (with mixed impedances).

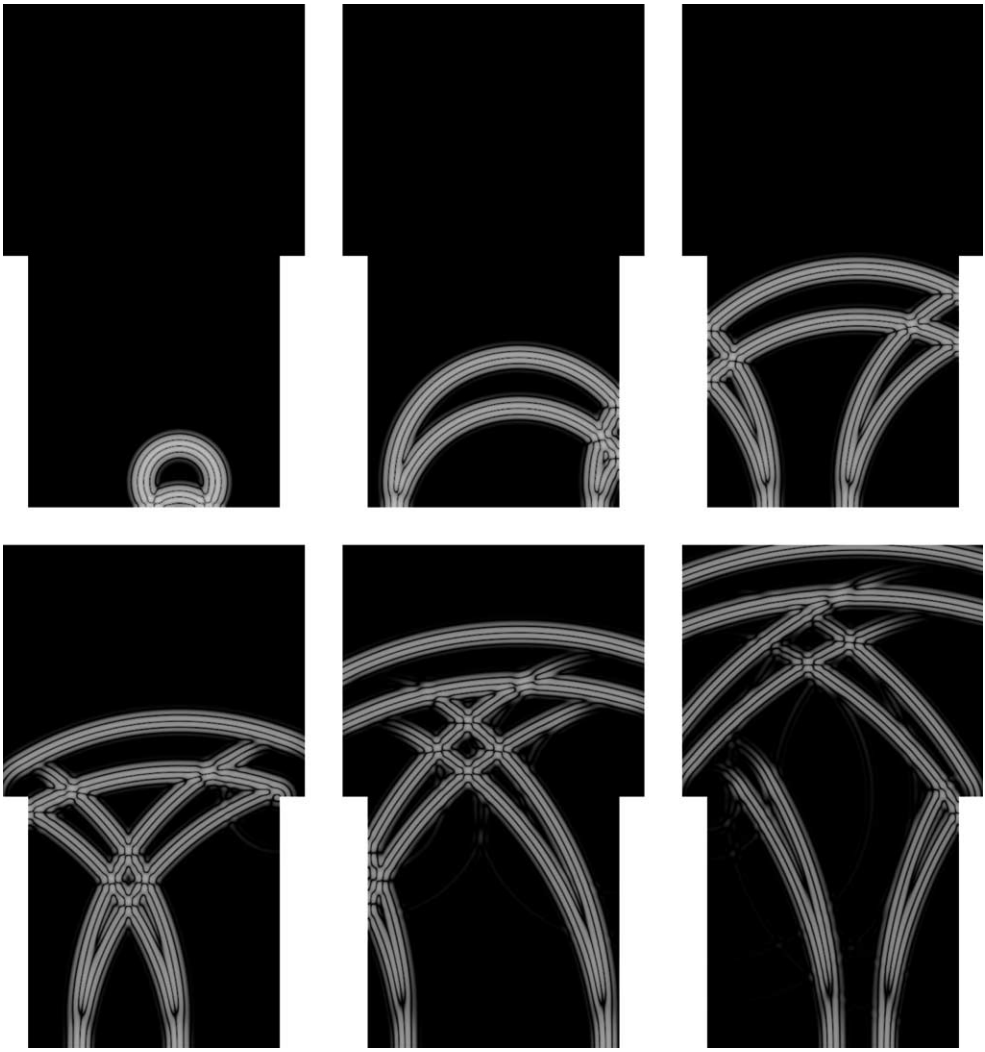

Fig. 10. Snapshots in the source canyon, in case of flat façades, at some selected times.

The effect of the impedance of the façades was already discussed in Section 3.5.2. Mixing rigid parts and partly reflecting parts results in sound pressure levels in between those of a uniform absorption. Results from the diffusely reflecting façade must be compared to the latter, in order to solely estimate the effect of non-flat walls. With increasing frequency, shielding increases. Starting from about 500 Hz, a gain in shielding of about 10 dB is observed. The diffusely reflecting façade that is modeled here results in a higher shielding than when simulating a flat façade with $Z = 10$, although an important part of the diffusely reflecting façade is rigid.

The main reason for this positive effect of a non-flat façade is a change in radiation pattern of the source canyon. With each reflection, part of the acoustical energy is reflected more upwardly and downwardly than in case of a flat façade. As a result, more acoustical

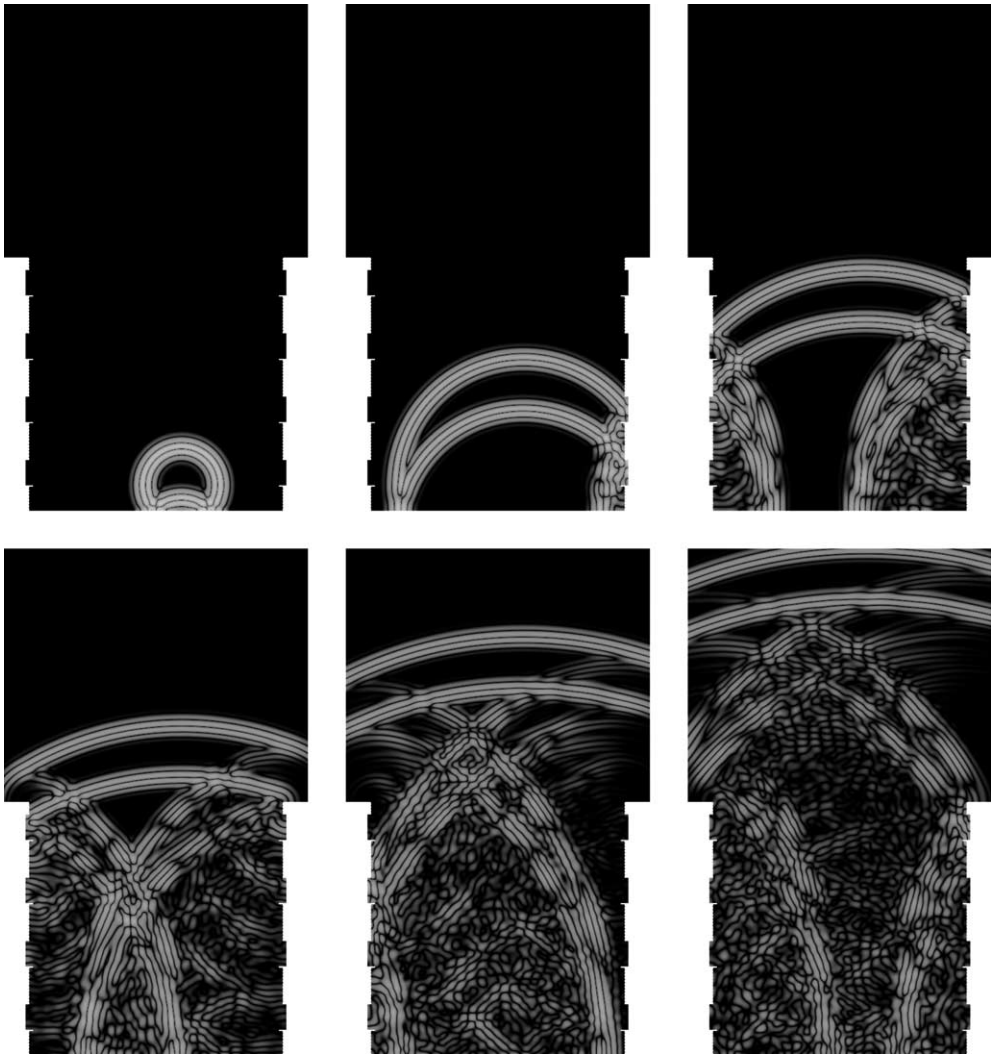

Fig. 11. Snapshots in the source canyon, in case of partly diffusely reflecting façades. Pressure fields are shown at exactly the same times as in Fig. 10.

energy is leaving the canyon in upward direction and waves arriving at the diffraction point on the middle building contain less energy.

### 3.5.4. Balconies

The presence of balconies near a façade is known to provide some acoustic protection. In [28], the optimal placement of absorbing material near balconies was investigated. Focus was on the protection of the façades in a source canyon. A 2D boundary element method was used in this study. The optimal and most practical place to apply absorbing material seemed to be the underside of the balconies.

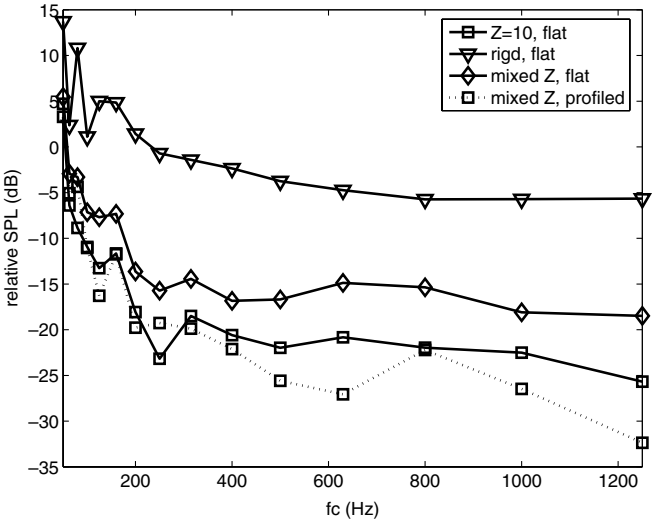


Fig. 12. Relative sound pressure levels in the receiver canyon, for completely flat façades (with a normalized impedance of 10, a rigid façade and a combination of these impedances as shown in Fig. 9), and for a partly diffusely reflecting façade (see profile in Fig. 8).

The influence of balcony depth and parapet inclination was studied in 3D on an 8-floor building, both with a ray-tracing method and on a scale model [29]. Increasing balcony width resulted in a somewhat decreased shielding at all floors, because of the increase in reflection on the underside of the upper balcony towards the underlying façade. Extra positive effects in the order of a few dB were obtained by inclining the parapets.

The effect of the presence of balconies in the street canyon, the inclination of the parapet and the placement of absorption on the underside of the balconies is modeled. In contrast to the cited publications in previous paragraph, we are interested in sound pressure levels in a nearby, shielded canyon. A balcony as shown in Fig. 13 is modeled. Three such balconies are placed near both façades in the source canyon. The undersides of the balconies are located at 2.5, 5 and 7.5 m from street level. Due to the symmetrical approach, the same balconies are present in the receiver canyon as well. The balcony width $D_b$ equals 0.5 m and the parapet height $H_b$ is 1 m. The thickness of the balcony floor and parapet $d_b$ is 0.2 m. A simulation is performed for a vertical parapet ($\alpha = 0°$) and for an inclination angle $\alpha$ of 30°. For the simulation with absorption, a (thin) material with impedance $Z = 5$ is placed along the full width ($d_b + D_b$) on the underside of the balconies.

The effect of the presence of balconies near the façades is shown in Fig. 14. Balconies increase shielding to an important degree in the receiver canyon. Especially at very low frequencies, the gain in shielding is remarkable. Reducing reflection on the undersides of the balconies has a rather limited effect on sound pressure levels in the shielded canyon.

Inclining the parapet results in some extra improvement compared to a vertical parapet, especially near 200–400 Hz. Although shielding in the current configuration is very sensitive to small changes in the geometry, the positive effect of parapet inclination holds in similar situations as well. In Fig. 15, the parapet inclination effect is checked in case of wider balconies ($D_b = 1$ m) and in case of shifting the balconies on the right-hand side of the street canyon by $-1.75$ m in vertical direction. The difference between shielding

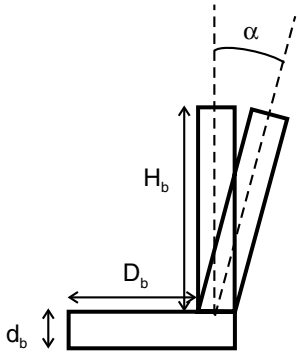


Fig. 13. Balcony form, with dimensions.

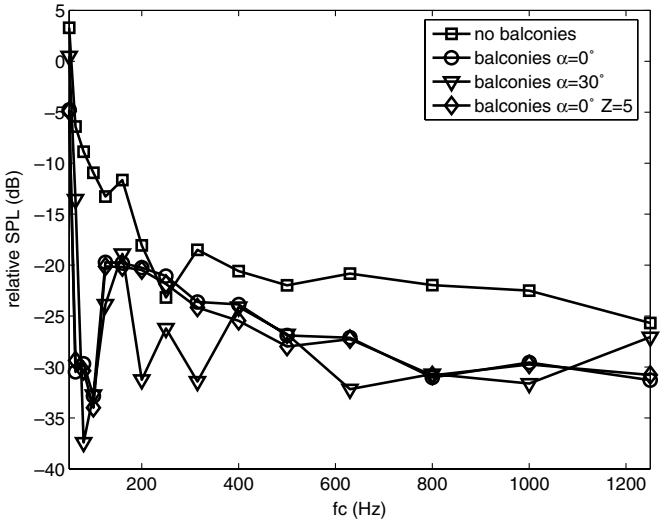


Fig. 14. Relative sound pressure levels in the receiver canyon, for a balcony with a straight parapet, an inclined parapet and in case of reduced reflection on the underside of the balconies. For comparison, the shielding in the standard configuration is shown as well.

in case of vertical and inclined parapets is explicitly shown. In case of placing wider balconies near both façades, the maximum effect is larger and shifted towards higher frequencies. Between 600 and 1000 Hz there are some (limited) negative effects as well by inclining parapets. When the balconies at the left and right façade do not appear at the same heights, the behavior is more or less similar to the symmetrical situation up to the 1/3 octave band of 250 Hz. Positive effects of inclination starting from 800 Hz are observed as well in the latter.

The effect of inclining the parapets can be attributed to a change in the complex interference patterns in the source canyons, altering the propagation towards the receiver at specific frequencies.

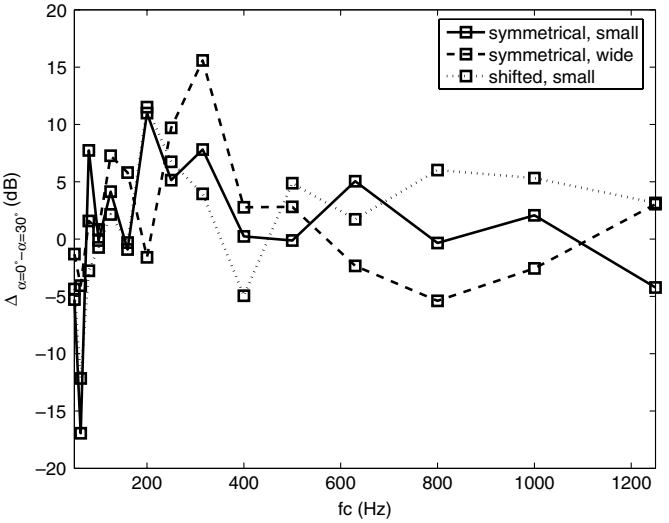


Fig. 15. Effect of inclining the parapets ($\alpha = 30°$) of the balconies near the façades, relative to vertical parapets. Small balconies ($D_b = 0.5$ m) and wider balconies ($D_b = 1$ m) are modeled in case of symmetrical façades. Small balconies that do not appear at the same heights at both façades (shifted) are simulated as well.

### 3.5.5. Moving atmosphere

The refraction which is present in an open field is enhanced by the interaction of the wind flow with buildings. This results in large gradients in the wind speed above the city canyons near roof level. This effect is more or less similar to the screen-induced refraction of sound by wind [13,30].

The wind flow above a city is highly turbulent. There is a large amount of advected turbulence in the flow due to the large number of interactions with obstacles upstream. It is possible to model a turbulent atmosphere with FDTD, as was done, e.g. in [31,32]. The computational cost of such calculations is however very large, since a sufficient number of simulations is necessary to obtain statistically relevant results. Therefore, turbulent scattering is modeled during the PE calculations only in our simulations. More information on this can be found in [24]. In the simulations where turbulent scattering is involved, an isotropic Von Kármán turbulence spectrum is used. The assumption of isotropy is however a simplification since increased turbulent strength can be expected near the edges of the buildings. Measurements of the turbulent strength from [33] were used as an estimate for the structure velocity parameter $C_v^2$ in our configuration. A value of $10\ m^{4/3}/s^2$ was used in case of $u^* = 1$ m/s. Since $C_v$ is proportional to $u^*$ [34], a value of $2.5\ m^{4/3}/s^2$ was used in case of the calmer wind. The correlation length was taken to be 10 m in both cases. Temperature turbulence is not accounted for.

The flow field in and around the canyon is calculated with CFD software Fluent [19]. A $k$–$\varepsilon$ turbulence model is used to account for the large, turbulent motions. A logarithmic inflow profile $u(z) = (u*/\kappa)\ln(1 + (z - 10)/z_0)$ is used (for $z \geqslant 10$ m), where $u^*$ is the friction velocity, $\kappa$ is the von Kármán constant ($\kappa = 0.4$), and $z_0$ is the ground roughness length. Positive values of the friction velocity correspond to downwind sound propagation from the source canyon to the receiver canyon, negative values to upwind sound propagation. Simulations are performed with $u^* = 0.5$ m/s, $u^* = 1$ m/s, $u^* = -0.5$ m/s and

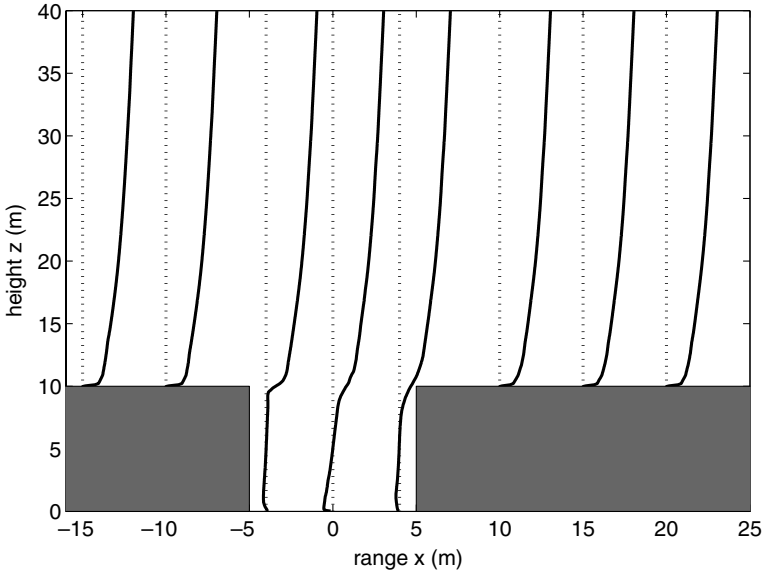


Fig. 16. Horizontal component of the flow velocity near the source canyon, in case of downwind sound propagation.

$u^* = -1$ m/s, while $z_0 = 0.5$ m. The flow velocity profiles near the source canyon for the standard configuration are shown in Fig. 16.

It can be seen from Fig. 17 that the wind effect is large. Downwind refraction becomes more pronounced with increasing frequency and with increasing wind speed. A decrease in

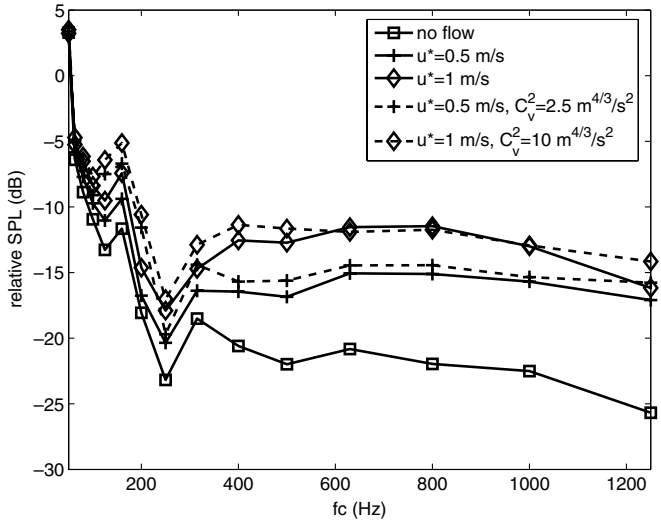


Fig. 17. Relative sound pressure levels in the receiver canyon, for downwind sound propagation. Two (inflow) wind speed profiles were used during the CFD calculations. The shielding in case of refraction, and in case of refraction combined with turbulent scattering is simulated. For comparison, the shielding in a non-moving atmosphere is shown as well.

shielding compared to a non-moving atmosphere near 10 dB is observed for $u^* = 1$ m/s, for frequency bands that are important for traffic noise. It is clear that the effect of wind cannot be neglected in these kinds of simulations. It can be seen in Fig. 17 that the wind effect increases some further when also accounting for a turbulent atmosphere. The main effect of the wind in case of downwind sound propagation is nevertheless refraction.

In case of upwind sound propagation, sound shielding increases with increasing wind speed. This is shown in Fig. 18. The very low sound pressure levels when using a friction velocity of $-1$ m/s will not be observed in practice, since high wind speeds are accompanied by turbulent scattering. The latter has shown to be very important. Almost no shielding is observed compared to calculations in a non-moving (non-turbulent) atmosphere. Including turbulent scattering in case of a lower wind speed leads to a somewhat decreased shielding compared to the sound propagation calculations in a non-moving atmosphere.

### 3.5.6. Distance between the canyons

The results in this parameter study are expressed relative to free field sound propagation calculations. This means that the figures shown in previous sections do not change with the distance between the canyons, unless the atmosphere is moving. Downwind sound propagation through a homogeneous, moving, non-turbulent atmosphere is modeled in Fig. 19. Simulations are performed for $D = 50$, 100 and 200 m. The same simulation parameters as in Section 3.5.5 are used.

With increasing distance, the sound pressure levels relative to the free field increase. In case of large values of $D$, more sound waves leaving the source canyon could be sufficiently bent downwards before reaching the receiver canyon. Therefore, the amount of acoustical energy refracted into the receiver canyon increases. When looking at absolute sound

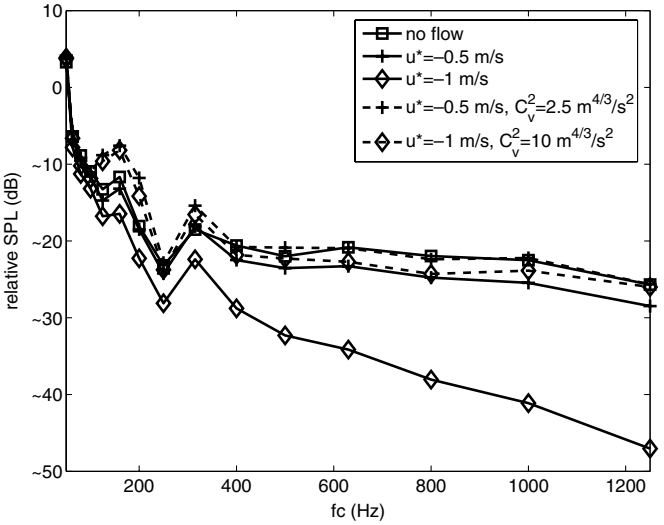


Fig. 18. Relative sound pressure levels in the receiver canyon, for upwind sound propagation. Two wind speed profiles were used during the CFD calculations. The shielding in case of refraction, and in case of refraction combined with turbulent scattering, is simulated. For comparison, the shielding in a non-moving atmosphere is shown as well.

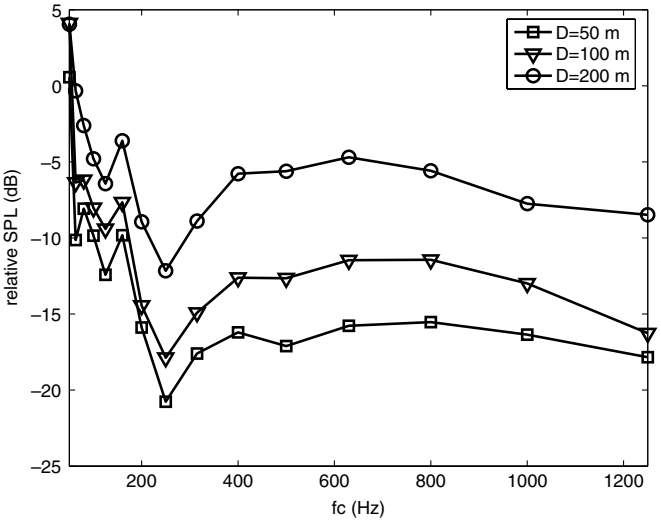


Fig. 19. Relative sound pressure levels in the receiver canyon, for downwind sound propagation (no turbulence). Three distances between the city canyons are considered.

pressure levels, the increase in wind effect is larger than the decrease in sound pressure level by geometrical spreading in our example.

### 3.5.7. Asymmetric source–receiver locations

In order to have an idea of the variation of shielding for different source–receiver positions, a number of calculations are performed. Ten locations ($x_s = x_r$, $z_s = z_r$) were

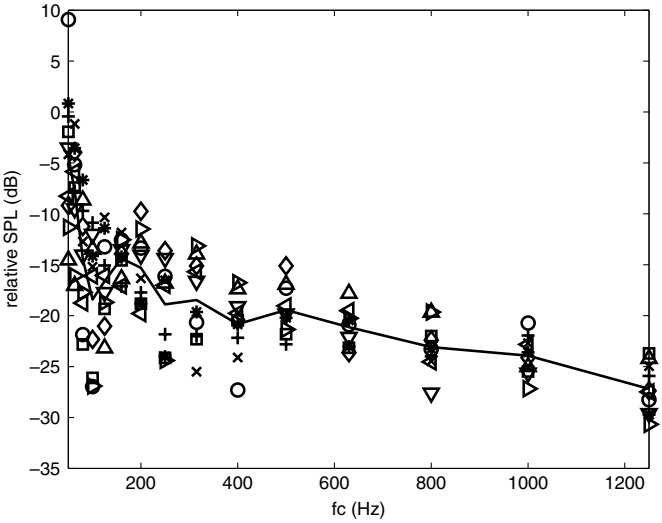


Fig. 20. Relative sound pressure levels in the receiver canyon, for various source/receiver locations. The mean values at each 1/3 octave band are connected with a full line.

considered namely (1 m, 1 m), (3 m, 1 m) (5 m, 1 m) (7 m, 1 m) (9 m, 1 m), (1 m, 2 m), (3 m, 2 m), (5 m, 2 m), (7 m, 2 m), (9 m, 2 m). This lead to 10 transfer functions from the source canyon to the receiver canyon, as shown in Fig. 20.

As can be expected, relative sound pressure levels vary significantly with source/receiver location. Variations are especially large for the low 1/3 octave bands.

We are however mainly interested in the relative effects of the investigated parameters, which is defined as the sound pressure level in a certain situation minus the sound pressure level in the standard configuration, for the same source/receiver location. Positive values indicate an increase in shielding, negative values a decrease in shielding.

In the symmetrical approach, the source location defines the receiver location, as described in Section 3.1. The relative effects of some configurations, applying the "symmetrical" approach, are compared to the relative effects in case of "asymmetric" source and receiver positions. In the latter, $x_s$ and $z_s$ must not be equal to $x_r$ and $z_r$. Such kind of simulations can only be performed with FDTD applied completely from the source to the receiver. Sound propagation from every source position, as defined above, is calculated towards all receiver positions in the receiver canyon, as defined above. Ten FDTD calculations were needed, leading to 100 transfer functions.

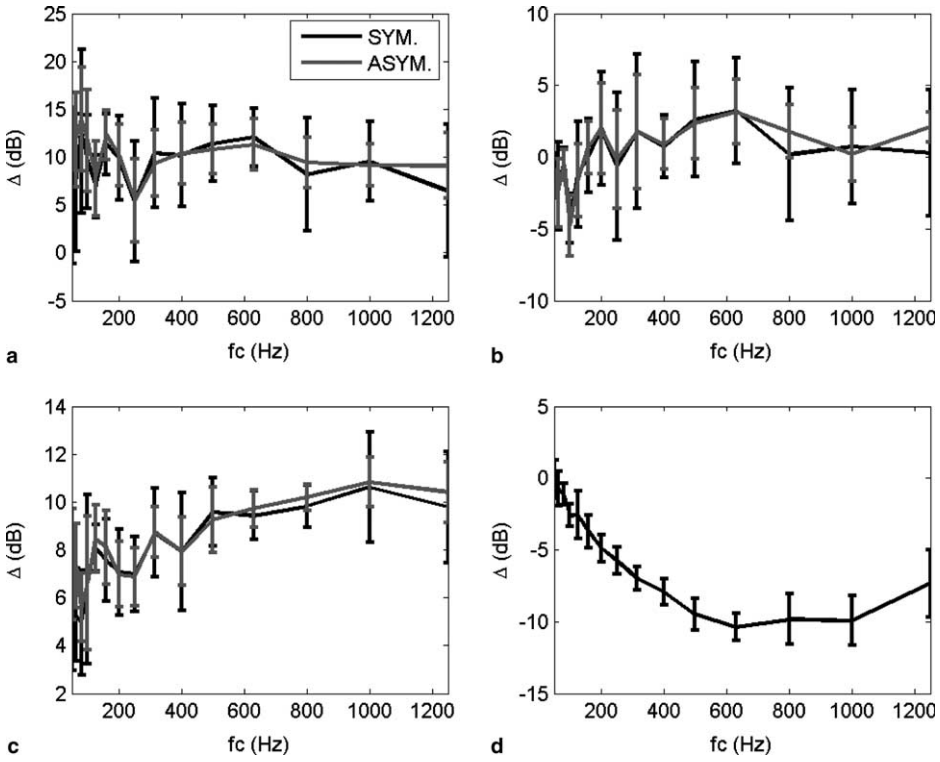


Fig. 21. Average relative effect of a certain case/geometry, in case of symmetrical and asymmetrical source–receiver locations. The standard configuration is taken as a reference. The error-bars have a total length of two times the standard deviation on the samples. In (a) the effect of $Z = 5$ is shown, in (b) the combined effect of a non-flat façade and wall impedance, in (c) the balcony effect, and in (d) the effect of downwind refraction.

Following relative effects were investigated:

- A normalized surface impedance at the façades of 5 (see Section 3.5.2).
- The profiled façade as described in Section 3.5.3.
- The balconies near the façades as described in Section 3.5.4, with an inclined parapet of 30°.
- The effect of downwind sound propagation with $u^* = 1$ m/s (see Section 3.5.5).

Results are shown in Fig. 21. The average effect over different source/receiver locations, relative to the standard configuration, is shown. The error-bars have a total length of 2 times the standard deviation on the samples. Asymmetric (or full) FDTD calculations in case (d) were not done because of the lack of sufficient computational resources. Note that the relative effect in Fig. 21(b) is a combination of non-flat façades and different wall impedances.

The average effect of a certain measure for the asymmetric calculations is very similar to the effects of the symmetric calculations. So the symmetric approach in this paper is sufficiently adequate to consider canyon to canyon propagation.

### 3.5.8. Combination of effects

The FDTD method allows combining various effects. In this way, realistic simulations are possible. As an example, the diffusely reflecting façade, as shown in Fig. 8, is combined with downwind refraction (with the inflow profile as described in Section 3.5.5 with $u^* = 1$ m/s). It can be seen from Fig. 22 that diffuse reflection and downwind refraction counteract. Diffuse reflection increases shielding, downwind refraction results in a decrease in shielding. The resulting shielding in this particular situation is very similar to the shield-

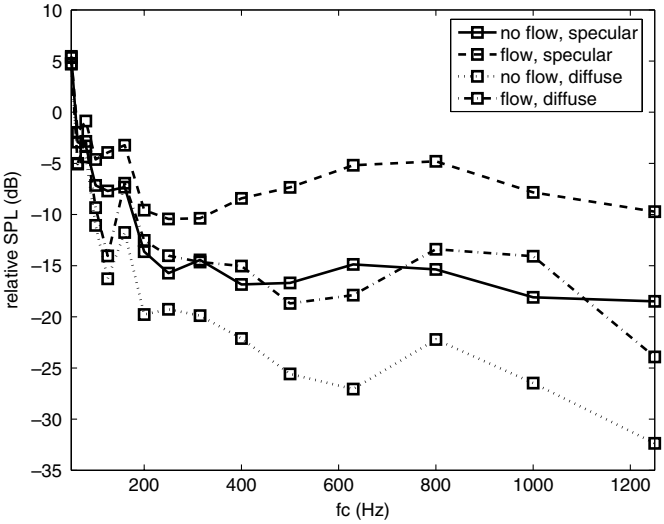


Fig. 22. Relative sound pressure levels in the receiver canyon, in case downwind sound propagation is combined with the non-flat façade profile shown in Fig. 8. For comparison, the shielding in a non-moving atmosphere with flat façades, a non-moving atmosphere with non-flat façades and a moving atmosphere with flat façade is shown as well. The flat façades have rigid and partly reflecting parts, as shown in Fig. 9.

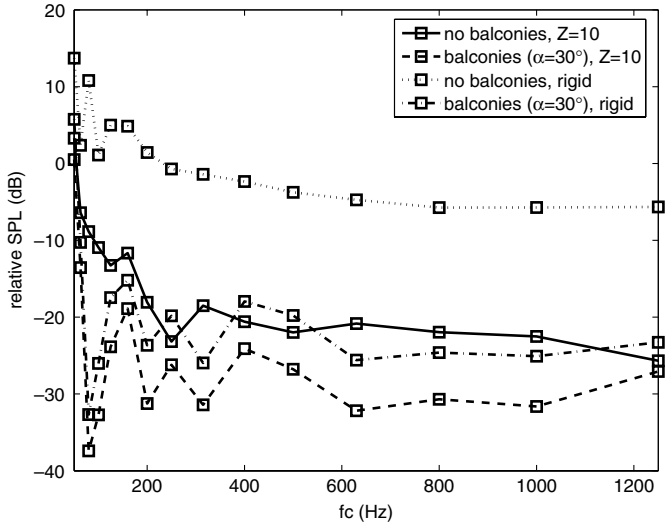


Fig. 23. Relative sound pressure levels in the receiver canyon, for a combination of balconies (with a parapet inclination $\alpha$ of 30°) and rigid façades. For comparison, the shielding in the standard configuration, in case of a rigid façade, and in case of the presence of balconies ($\alpha = 30°$) with $Z = 10$ is shown as well.

ing obtained in a non-moving atmosphere, with a flat façade. Both effects are more or less additive.

In another example, rigid façades are compared to façades with balconies with an inclined parapet of 30°, as described in Section 3.5.4. This is shown in Fig. 23. Adding the relative effects of both the rigid façade and the balconies would largely underestimate the shielding. It can therefore be concluded that numerical simulations will be necessary to estimate the effect of combinations of parameters.

## 4. Conclusion

In this paper, a parameter study has been described for the case of two-dimensional sound propagation from a source canyon to a nearby, identical receiver canyon. A coupled FDTD-PE model was applied. Symmetry of the source and receiver canyon allowed calculating in only half the sound propagation domain. Very good agreement was obtained between the coupled FDTD-PE model, exploiting symmetry, and reference calculations (i.e., FDTD applied completely from source to receiver). Focus was on the sound pressure levels in the receiver canyon. Although the general applicability of this model in urban areas is limited, the FDTD-PE model is well suited and numerically efficient in prototype situations and thus allows investigating the effect of important parameters.

Working in a two-dimensional simulation space means that a coherent line source is modeled. The effect of an incoherent line source, which is more appropriate for traffic noise, is estimated by performing a number of calculations in 2D cross-sections through source and receiver. Modeling an incoherent line source resulted in a decrease in shielding compared to a coherent line source. Expressing results in 1/3 octave bands however already averaged out to some degree the deep destructive interferences that arise when working with a coherent line source.

The shielding was found to be rather insensitive to the width-height ratio of the canyons, except for very narrow canyons. For ratios larger than 1, relative sound pressure levels at the receiver become more or less constant. The degree of absorption on the façades is very important, due to the large number of interactions between the sound waves and the walls. Rigid walls result in very poor shielding towards the receiver canyon. With the FDTD code it is possible to simulate well-localized diffusers near the façades. The effect of introducing recesses by windows and protrusions by windowsills, together with a roughened wall, increases with increasing frequency when comparing to flat façades. Near 1000 Hz, about 10 dB in shielding is gained for the profiled façade that was simulated in this paper. It has to be mentioned that scattering is only simulated in two dimensions. The presence of balconies resulted in an important increase in shielding. Especially near very low 1/3 octave bands, a large increase in shielding is obtained. Inclining the parapet of the balconies resulted in an extra increase at some frequency bands.

The effect of a moving atmosphere was investigated in detail. Flow calculations near the canyons were performed, and this information was used during the sound propagation calculations. In case of downwind sound propagation, shielding decreases to an important degree compared to a non-moving atmosphere. Refraction is the most important effect in the latter. With increasing incident wind speed and with increasing frequency, shielding decreases. In case of upwind sound propagation, turbulent scattering plays an important role and the shielding does not increase compared to a non-moving atmosphere in our calculation.

Symmetrical source–receiver locations were shown to be suited to estimate effects of asymmetric source–receiver locations as well. Examples showed that the combined effect of parameters is in general not simply the addition of the separate effects.

## Acknowledgments

The authors would like to thank Tom De Muer (from Ghent University, Department of Information Technology) for helpful comments on this paper.

## References

[1] Heutschi K. A simple method to evaluate the increase of traffic noise emission level due to buildings for a long straight street. Appl Acoust 1995;44:259–74.
[2] Lu K, Li K. The propagation of sound in narrow street canyons. J Acoust Soc Am 2002;112:537–50.
[3] Kang J. Numerical modelling of the sound fields in urban streets with diffusely reflecting boundaries. J Sound Vibr 2002;258:793–813.
[4] Kang J. Sound propagation in street canyons: Comparison between diffusely and geometrically reflecting boundaries. J Acoust Soc Am 2000;107:1394–404.
[5] Picault J. Numerical modeling of urban sound fields by a diffusion process. Appl Acoust 2002;63:965–91.
[6] Le Polles T, Picault J, Berengier M. Sound field modeling in a street canyon with partially diffusely reflecting boundaries by the transport theory. J Acoust Soc Am 2004;116:2969–83.
[7] Öhrström E. Psycho-social effects of traffic noise exposure. J Sound Vibr 1991;151:513–7.
[8] Kihlman T. Quiet side and high façade insulation – means to solve the city noise problem. In: Proceedings of internoise 2001, The Hague, The Netherlands.
[9] Kihlman T, Ögren M, Kropp W. Prediction of urban traffic noise in shielded courtyards. In: Proceedings of internoise 2002, Dearborn, MI, USA.
[10] Ögren M, Kropp W. Road traffic noise propagation between two dimensional city canyons using an equivalent sources approach. Acta Acustica united with Acustica 2004;90:293–300.

[11] Ögren M, Forssen J. Modeling a city canyon problem in a turbulent atmosphere using an equivalent sources approach. Appl Acoust 2004;65:629–42.
[12] Blumrich R, Heimann D. A linearized Eulerian sound propagation model for studies of complex meteorological effects. J Acoust Soc Am 2002;112:446–55.
[13] Van Renterghem T, Botteldooren D. Numerical simulation of the effect of trees on downwind noise barrier performance. Acta Acustica united with Acustica 2003;89:764–78.
[14] Ostashev V, Wilson D, Liu L, Aldridge D, Symons N, Marlin D. Equations for finite-difference, time-domain simulation of sound propagation in moving inhomogeneous media and numerical implementation. J Acoust Soc Am 2005;117:503–17.
[15] Horoshenkov K, Hothersall D, Mercy S. Scale modelling of sound propagation in a city street canyon. J Sound Vibr 1999;223:795–819.
[16] Van Renterghem T, Salomons E, Botteldooren D. Efficient FDTD-PE model for sound propagation in situations with complex obstacles and wind profiles. Acta Acustica united with Acustica 2005;91:671–9.
[17] Thorsson P, Ögren M, Kropp W. Noise levels on the shielded side in cities using a flat city model. Appl Acoust 2004;65:313–23.
[18] Botteldooren D. Finite-difference time-domain simulation of low-frequency room acoustic problems. J Acoust Soc Am 1995;98:3302–8.
[19] Fluent, Computational Fluid Dynamics Software, version 6, Fluent, Incorporated, Centerra Resource Park, 10 Cavendish Court, Lebanon, NH 03766.
[20] Van Renterghem T, Botteldooren D, Salomons E. Efficiency of FDTD and hybrid techniques for outdoor sound propagation modeling. In: Proceedings of long range sound propagation symposium 2004, Fairlee, VT, USA.
[21] Van Renterghem T, Botteldooren D. Prediction-step staggered-in-time FDTD: an efficient numerical scheme to solve the linearised equations of fluid dynamics in outdoor sound propagation. Appl Acoust (accepted).
[22] Gilbert K, Di X. A fast Green's function method for one-way sound propagation in the atmosphere. J Acoust Soc Am 1993;94:2343–52.
[23] Salomons E. Improved Green's function parabolic equation method for atmospheric sound propagation. J Acoust Soc Am 1998;104:100–11.
[24] Salomons E. Computational atmospheric acoustics. Dordrecht: Kluwer Academic Publishers; 2001.
[25] Salomons E. Sound propagation in complex outdoor situations with a non-refracting atmosphere: model based on analytical solutions for diffraction and reflection. Acta Acustica united with Acustica 1997;83:436–54.
[26] Heutschi K, Horvath M, Hofmann J. Simulation of ground impedance in finite difference time domain calculations of outdoor sound propagation. Acta Acustica united with Acustica 2005;91:35–40.
[27] Ismail M, Oldham D. A scale model investigation of sound reflection from building façades. Appl Acoust 2005;66:123–47.
[28] Hothersall D, Horoshenkov K, Mercy S. Numerical modelling of the sound field near a tall building with balconies near a road. J Sound Vibr 1996;198:507–15.
[29] Hossam El Dien H, Woloszyn P. The acoustical influence of balcony depth and parapet form: experiments and simulations. Appl Acoust 2005;66:533–51.
[30] Salomons E. Reduction of the performance of a noise screen due to screen-induced wind-speed gradients. Numerical computations and wind tunnel experiments. J Acoust Soc Am 1999;105:2287–93.
[31] Heimann D, Blumrich R. Time-domain simulations of sound propagation through screen-induced turbulence. Appl Acoust 2004;65:561–82.
[32] Symons N, Aldridge D, Marlin D, Wilson D, Patton E, Sullivan P, et al. 3D Staggered-grid finite-difference simulation of sound refraction and scattering in moving media. In: Proceedings of 11th international symposium on long range sound propagation 2004, Fairlee, VT, USA.
[33] Forssen J, Ögren M. Thick barrier noise-reduction in the presence of atmospheric turbulence: measurements and numerical modeling. Appl Acoust 2002;63:173–87.
[34] Wilson D. A turbulence spectral model for sound propagation in the atmosphere that incorporates shear and buoyancy forcings. J Acoust Soc Am 2000;108:2021–38.